Am J Physiol Lung Cell Mol Physiol 316: L1107–L1117, 2019.
First published March 20, 2019; doi:10.1152/ajplung.00391.2018.

RESEARCH ARTICLE

Prophylactic treatment with MSC-derived exosomes attenuates traumatic acute lung injury in rats

Qing-Chun Li,[1] Yun Liang,[2] and Zhen-Bo Su[3]

[1]*Department of Gastrointestinal Colorectal and Anal Surgery, China-Japan Union Hospital of Jilin University, Changchun, People's Republic of China;* [2]*Center of Physical Examination, China-Japan Union Hospital of Jilin University, Changchun, People's Republic of China; and* [3]*Department of Anesthesiology, China-Japan Union Hospital of Jilin University, Changchun, People's Republic of China*

Submitted 22 August 2018; accepted in final form 15 March 2019

Li QC, Liang Y, Su ZB. Prophylactic treatment with MSC-derived exosomes attenuates traumatic acute lung injury in rats. *Am J Physiol Lung Cell Mol Physiol* 316: L1107–L1117, 2019. First published March 20, 2019; doi:10.1152/ajplung.00391.2018.—The mesenchymal stem cell (MSC) is a potential strategy in the pretreatment of traumatic acute lung injury (ALI), a disease that causes inflammation and oxidative stress. This study aimed to investigate whether MSC-exosomal microRNA-124-3p (miR-124-3p) affects traumatic ALI. Initially, a traumatic ALI rat model was established using the weight-drop method. Then, exosomes were obtained from MSCs of Sprague-Dawley rats, which were injected into the traumatic ALI rats. We found that miR-124-3p was abundantly-expressed in MSCs-derived exosomes and could directly target purinergic receptor P2X ligand-gated ion channel 7 (P2X7), which was overexpressed in traumatic ALI rats. After that, a loss- and gain-of-function study was performed in MSCs and traumatic ALI rats to investigate the role of miR-124-3p and P2X7 in traumatic ALI. MSC-derived exosomal miR-124-3p or silenced P2X7 was observed to increase the survival rate of traumatic ALI rats and enhance the glutathione/superoxide dismutase activity in their lung tissues. However, the wet/dry weight of lung tissues, activity of methylenedioxyamphetamine and H_2O_2, and levels of inflammatory factors (TNF-a, IL-6, and IL-8) were reduced. Similarly, the numbers of total cells, macrophages, neutrophils, and lymphocytes in bronchoalveolar lavage fluid were also reduced when treated with exosomal miR-124-3p or silenced P2X7. In conclusion, the results provide evidence that miR-124-3p transferred by MSC-derived exosomes inhibited P2X7 expression, thus improving oxidative stress injury and suppressing inflammatory response in traumatic ALI, highlighting a potential pretreatment for traumatic ALI.

exosomes; inflammatory response; mesenchymal stem cells; microRNA-124-3p; oxidative stress injury; purinergic receptor P2X ligand-gated ion channel 7; traumatic acute lung injury

INTRODUCTION

Traumatic injury exaggerated the response of the immune system to subsequent infectious attacks, in which the lung is a particularly fragile organ (18). Traumatic acute lung injury (ALI) is characterized by oxidative stress (OS) injury and inflammatory responses, which may lead to mortality (19). Inflammation has been reported to play essential roles in traumatic brain injury (TBI)-induced ALI (24). Currently, conventional mechanical ventilation remains to be a supportive regimen designed to support respiratory function for ALI (1). However, pretreatment for ALI patients was still needed to be investigated. Strikingly, mesenchymal stem cells (MSCs) have been reported to contribute to tissue repair and participate in pulmonary fibrosis (9, 43). MSCs are potential tools for the treatment of lung diseases and may play a role in traumatic ALI, but the specific nature and reliability remain unclear. In the rat model of pulmonary contusion, MSCs may ameliorate stress-induced wound healing injury (14). Moreover, it has been proven that the protective effect of fibroblast growth factor-10 on ALI might be mediated by the mobilization of lung-resident MSCs (40).

As shown in previous studies, exosomes can be derived from MSCs (30, 37). Exosomes have the ability to carry lipid mediators, microRNAs (miRs), and various types of proteins (47). miRs play vital roles in cell proliferation, apoptosis, and differentiation throughout the human body (23). miR-124-3p has been reported to be enriched in the brain and participate in the development of cranial and spinal nerves (42). Besides, miR-124-3p also plays a vital role in inhibiting the development of tumors by binding to different genes. Furthermore, it has been suggested that miR-124-3p could contribute to anti-inflammation via its interactions with Toll-like receptor 3 (20). Intriguingly, exosomes derived from miR-124-3p-overexpressing microglia exerted an anti-inflammatory effect on TBI (21). Furthermore, in the current study, it has been confirmed that miR-124-3p could target purinergic receptor P2X ligand-gated ion channel 7 (P2X7) based on results of dual luciferase assay. As one of the purinergic receptors, P2X7 is closely involved in the human inflammatory and stress responses (10). A previous study revealed that P2X7 can serve as a potential target in the treatment of inflammatory diseases (5). In addition, overexpression of P2X7 could upregulate the levels of proinflammatory cytokines including interleukin (IL)-6 and tumor necrosis factor (TNF)-α (38). Moreover, downregulation of P2X7 was revealed to exert protective effects against ALI by suppressing inflammation (11). However, the specific molecular mechanism by which MSCs act in lung diseases remains unclear. Based on the above findings, we hypothesize that MSCs as a preventative strategy are involved in OS and inflammation induced by traumatic ALI through regulating P2X7 expression by secreting exosomes to transfer miR-124-3p.

Address for reprint requests and other correspondence: Z.-B. Su, Department of Anesthesiology, China-Japan Union Hospital of Jilin University, No. 126, Xiantai Street, Changchun 130033, Jilin Province, P.R. China (e-mail: suzb@jlu.edu.cn).

MATERIALS AND METHODS

Ethics statement. This current study was carried out in strict accordance with the recommendations in the *Guide for the Care and Use of Laboratory Animals*. The principle of completing experiments using the minimum number of animals was performed with the best efforts to minimize the suffering of the included animals. All experimentation protocols were approved and followed the Ministry of Science and Technology of the People's Republic of China on the Guiding Opinions on Treating Experimental Animals [National Science and Technology (2006) No. 398] and the National Institutes of Health *Guide for the Care and Use of Laboratory Animals* (Publication No. 85-23, revised 1996).

Experimental animals. A total of 212 4-mo-old healthy specific pathogen-free (SPF) male Sprague-Dawley (SD) rats (weighing 180–230 g) were obtained from the Experimental Animal Center of Jilin University. Ten of the included rats were used for isolation and culture of MSCs.

Isolation, culture, and differentiation of MSCs. The tibia and femur of two SD rats were obtained and the connective and muscle tissues were removed. The ends of the bone were cut by scissors, and the bone marrow cavity was flushed with serum-free medium containing Dulbecco's modified Eagle's medium (DMEM) for cell suspension preparation. The prepared cell suspension was then centrifuged at 900 *g* for 5 min. After that, the cell suspension was resuspended at a concentration of $10^5/cm^2$ in DMEM containing 10% FBS (Hangzhou Sijiqing Biological Engineering Materials, Hangzhou, China), 100 U/ml penicillin, and 100 μg/ml streptomycin (Gibco, Carlsbad, CA). Next, the cell suspension was cultured at 37°C with 5% CO_2 and passaged for future use. The obtained MSCs (2.5×10^5) were subjected to induction of chondrogenic and adipogenic differentiation (51).

Isolation and identification of MSC-derived exosomes. When cell confluence reached 90%, MSCs were rinsed twice with 1 × PBS and resuspended in 15 ml serum-free medium. MSCs were then incubated at 37°C for 48 h in a humidified incubator with 94% N_2-1% O_2-5% CO_2 in air. Then, the supernatant was collected and mixed with exosome extractant (Ribobio, Guangzhou, China) at a ratio of 3: 1. After that, the supernatant was centrifuged at 4°C at 2,000 *g* for 15 min, at 5,000 *g* for 15 min, at 12,000 *g* for 30 min, and at 12,000 *g* for 70 min, respectively, to collect the exosomes, which were then stored at −80°C for further experimentation.

The exosomes were then fixed in 4% glutaraldehyde for 2 h at 4°C and rinsed by 0.1 mol/l PBS three times. After a further fixation in 1% osmium tetroxide for 2 h, the exosomes were dehydrated by conventional ethanol and gradient acetone. After that, the exosomes were impregnated, embedded, and polymerized with ethoxyline resin, followed by preparation of 0.5-μm semi-thin sections. Then, the semi-thin sections were cut into 60-nm ultrathin sections under a light microscope. After that, the sections were stained with uranium acetate and lead citrate and observed under a transmission electron microscope (JEM-1400, 120 KV; JEOL, Tokyo, Japan). The size and concentration of exosomes were determined by the nanoparticle tracking analysis, and the expression of the protein surface biomarkers (CD63, CD9, and CD81) in the exosomes were measured by Western blot analysis. Furthermore, a bicinchoninic acid assay (Thermo Fisher Scientific, Waltham, MA) was used to detect the protein concentration of the exosomes (27, 28, 31). About 25 μg of exosomes were obtained from 2×10^7 MSCs.

Establishment of traumatic ALI rat model. This study is a separate pilot series. The rest 210 rats were adaptively fed in a clean-grade animal room for 7 days at temperatures between 20 and 25°C with a controlled day-night alterations and were allowed free access to food and water. After that, 15 rats were used as normal controls (the normal group) and the other 195 rats were established as ALI models. For ALI model establishment (19), rats were intraperitoneally anesthetized using 2% pentobarbital sodium (30 mg/kg) (19), fixed, and placed on an experimental platform for stimulation chest trauma conditions. After that, the chest of the rats was struck by a 200-g stainless hammer placed 100 cm away from the platform (19). Then, 45 ALI rats were prepared for exosome experimentation, and 150 for exosome/miR-124-3p/P2X7 experimentation. After being fasted for 12 h, the 45 rats selected for exosome research were assigned into the following groups (15 rats in each group) with different treatment: the ALI group, the ALI + PBS group, and the ALI + exosomes group. Rats in the ALI + PBS group were injected with 100 μl PBS through the caudal vein 30 min before model establishment. Rats in the ALI + exosomes group were injected with 100 μl PBS containing 25 μg of exosomes through the caudal vein 30 min before model establishment. After model establishment, to evaluate whether the ALI model was successfully established or not, we measured the arterial oxygenation index (Pa_O/Fi_O, ≤300 mmHg) and dry/wet weight ratio of lung tissues (to determine the degree of lung injury and edema) of rats, observed histopathological characteristics of lung, and performed a pathological score of traumatic ALI (33).

Transfection of MSCs. MSCs were classified into the following groups: the oe-negative control (NC) group, the oe-miR-124-3p group, the sh-NC group, and the sh-miR-124-3p group. Overexpressed plasmid vectors and interference plasmid vectors of lentivirus (Invitrogen, Carlsbad, CA) were constructed. For transfection (21), MSCs (5.0×10^7/ml) were seeded into a six-well plate with 2 ml/well and incubated with the prepared lentiviral supernatant (with a higher concentration than 10^7 TU/ml) when cell confluence reached 50%. Following a 24-h period of transfection, the solution was replaced with a complete medium. When cell confluence reached 80%, the complete medium was replaced with a serum-free medium for further 24-h incubation. Then, the exosomes were isolated by the differential centrifugation. The expression of miR-124-3p in the isolated exosomes was detected by reverse transcription-quantitative polymerase chain reaction (RT-qPCR) and compared with that of exosomes isolated from nontransfected MSCs.

Grouping and treatment of traumatic ALI rat models. The prepared 150 ALI rats used for exosome/miR-124-3p/P2X7 experiment were classified into the following 10 groups (15 rats/group): the vector-NC group (rats injected with 10 μl lentiviruses), the P2X7-vector group (rats injected with 10 μl lentiviruses), the si-NC group (rats injected with 10 μl lentiviruses), the si-P2X7 group (rats injected with 10 μl lentiviruses), the oe-NC group (rats injected with 100 μl PBS containing 25 μg exosomes), the oe-miR-124-3p group (rats injected with 100 μl PBS containing 25 μg exosomes), the sh-NC group (rats injected with 100 μl PBS containing 25 μg exosomes), the sh-miR-124-3p group (rats injected with 100 μl PBS containing 25 μg exosomes) (3), the oe-miR-124-3p + vector-NC group (rats injected with 100 μl PBS containing 25 μg exosomes and 10 μl vector-NC), and the oe-miR-124-3p + P2X7-vector group (rats injected with 100 μl PBS containing 25 μg exosomes and 10 μl P2X7-vector). The injection of PBS containing 25 μg exosomes was repeated every 2 days after model establishment (2). At last, the rats in each group were fed with a common diet with free access to water, and the feeding room was guaranteed for a 12:12-h light-dark cycle each day.

Survival analysis. During 0~120 h, the survival curves of rats were drawn using the Kaplan-Meier method. After 7 days, five surviving rats in each group (5–10 rats died in each group) were used for subsequent experimentation.

Measurement for wet-to-dry ratio of lung tissues. Following a 7-day period, the rats were anesthetized with 2% sodium pentobarbital. After removal of the blood on the surface, the wet weight of the lungs was measured using an analytical balance. After that, the lungs were dehydrated at 80°C for 48 h to measure the dry weight. W/D was calculated as the ratio of wet weight to the dry weight.

Hematoxylin-eosin staining for lung tissues. The right lung tissues were fixed in 10% neutral formalin solution and prepared as tissue sections. After routine hematoxylin-eosin staining, the sections were sealed by neutral balsam to observe the histopathological changes

Table 1. *Primer sequences for RT-qPCR*

Gene	Primer Sequence
miR-124-3p	
Forward	5′-UAAGGCACGCGGUGAAUGCC-3′
Reverse	5′-GCATTCACCGCGUGCCUUAUU-3′
U6	
Forward	5′-AACGCTTCACGAATTTGCGT-3′
Reverse	5′-CTCGCTTCGGCAGCACA-3′
P2X7	
Forward	5′-CGGGCCACAACTATACTACGA-3′
Reverse	5′-CCTGAACTGCCACCTCTGTAA-3′
GAPDH	
Forward	5′-CCCTTCATTGACCTCAACTACATG-3′
Reverse	5′-CTTCTCCATGGTGGTGAAGAC-3′
miR-409b	
Forward	5′-GCGAATGTTGCTCGGTGA-3′
Reverse	5′-GTGCAGGGTCCGAGGT-3′
miR-149-3p	
Forward	5′-CCTTTGACTGCCGTGCGT-3′
Reverse	5′-CCGTCAGCCACCTCTCAC-3′
miR-1956-5p	
Forward	5′-ACACTCCAGCTGGGAGTCCAGGGCTGAGTC-3′
Reverse	5′-AGUCCAGGGCUGAGUCAGCGGATCCGCTGA-3′

GAPDH, glyceraldehyde-3-phosphate dehydrogenase; P2X7, purinergic receptor P2X7; miR, microRNA; RT-qPCR, reverse transcription-quantitative polymerase chain reaction.

under a light microscope and score the pathological injuries according to the reference (17) by two pathologists by the double-blind method. The experiment was repeated three times.

Inflammatory cell counting and protein content determination. The bronchoalveolar lavage fluid (BALF) was collected from rats using PBS, which was then centrifuged. After being resuspended in normal saline, the total cell number was counted using a hemocytometer, and the number of different cells was counted under a light microscope after being staining with a Wright-Gimsa staining kit (Jiancheng, Nanjing, China). The total protein content in BALF was determined by a semiautomated spectrophotometer kit (Labtest Diagnóstica, Minas Gerais, Brazil).

Oxidative stress. The activity of superoxide dismutase (SOD), malondialdehyde (MDA), H_2O_2, and glutathione (GSH) were all measured using the manufacturer's instructions (Jiancheng), and the experiment was repeated three times.

Enzyme-linked immunosorbent assay. The levels of inflammatory factors including TNF-α, IL-6, IL-8, and IL-10 in BALF were detected by enzyme-linked immunosorbent assay (ELISA) kits according to the manufacturer's instructions (Wuhan Cusabio Biotech, Wuhan, China). The experiment was repeated three times.

RT-qPCR. The total RNA was extracted using Trizol (Invitrogen, Carlsbad, CA), and the concentration was determined by Nanodrop 2000 (Thermo Fisher Scientific). For RT-qPCR, 1 μg of total RNA was reverse transcribed into complementary DNA (cDNA) using the PrimeScript RT reagent kit and gDNA Eraser kit (Takara Holdings, Kyoto, Japan). Then, RT-qPCR was performed on an ABI7500 quantitative PCR instrument (Thermo Fisher Scientific) using the SYBR Premix Ex Taq (Tli RNaseH Plus) kit (Takara Holdings). U6 was regarded as the internal reference for miR, and GAPDH for P2X7. The $2^{-\Delta\Delta Ct}$ method was used for quantification of relative expression (25). Primers used in this experiment are displayed in Table 1 and were all synthesized by Shanghai GenePharma (Shanghai, China).

Western blot analysis. Total protein of lung tissues was extracted using the RIPA containing PMSF (R0010; Beijing Solarbio Science and Technology, Beijing, China), and the protein concentration was determined using a bicinchoninic acid kit (Thermo Fisher Scientific). Then, proteins were separated using SDS-PAGE and transferred onto PVDF membrane (Amersham, GE Healthcare, Chicago, IL). After being blocked with 5% skim milk powder for 1 h at room temperature, the membrane was incubated with the following rabbit polyclonal primary antibodies at 4°C overnight purchased from Abcam (Cambridge, UK): anti-P2X7 (1:1,000, ab48871), anti-CD9 (1:2,000, ab92726), anti-CD81 (1:1,000, ab109201), and anti-CD63 (1:500, ab108950), with mouse monoclonal anti-GAPDH antibody (1:10,000, ab8245) as the internal reference. Then, the membrane was incubated with goat anti-rabbit secondary antibody (1:10,000; Jackson ImmunoResearch, West Grove, PA) for 1 h at room temperature. Next, the membrane was developed using an ECL reaction solution (WBKLS0100; Millipore, Bedford, MA) and exposed on an optical luminometer (GE Healthcare). The relative expression of proteins was analyzed using the Protein Pro Plus 6.0 software (Media Cybernetics, Rockville, MD). The experiment was repeated three times.

Bioinformatics analysis. P2RX7 was used as the key word for searching the regulatory miRs of P2X7 in three miR-mRNA relationship prediction sites, including miRDB (http://www.mirdb.org/), Target Scan (http://www.targetscan.org/vert_71/), and miRWalk (http://mirwalk.umm.uni-heidelberg.de/). The jvenn website (http://jvenn.toulouse.inra.fr/app/example.html) was used to compare the predicted results obtained from the above websites.

Dual luciferase reporter gene assay. Wild type (WT) and mutant (MUT) of 3′-untranslated region gene fragments of miR (miR-124-3p) were artificially synthesized and presented to the pMIR-reporter (Beijing Huayueyang Biotechnology, Beijing, China) by the endonuclease sites SpeI and Hind III. The target fragment was inserted into the pMIR-reporter plasmid through T4 DNA ligase by the restriction endonuclease digestion. After insertion, the correctly sequenced luciferase reporter plasmids (WT and MUT) were cotransfected with miR onto HEK-293T cells (Shanghai Beinuo Life Science, Shanghai, China) respectively. Following a 48-h period of transfection, HEK-293T cells were collected and lysed to measure the luciferase activity by a luciferase assay kit (K801-200; BioVision, San Francisco, CA) and a Glomax 20/20 luminometer fluorescence detector (Promega, Madison, WI). Each experiment was repeated three times.

Statistical analysis. All data are expressed as means ± SD and were tested for normal distribution and homogeneity variance. Statistical analyses were performed using SPSS 21.0 statistical software (IBM, Armonk, NY). Comparisons between two groups were analyzed by the unpaired Student's *t*-test, whereas one-way ANOVA was used for comparisons among multiple groups. A Tukey test was used for post hoc test. The survival rate of rats was analyzed by Kaplan-Meier analysis. $P < 0.05$ was considered to be statistically significant.

RESULTS

Morphological changes in MSCs. At 7 days after inoculation, a large number of elongated primary MSCs were observed (Fig. 1*A*). After induction of chondrogenic differentiation, the volume of MSCs was increased and attained elliptical or kidney shapes (Fig. 1*B*). After induction of osteogenic differentiation, numerous dense calcium nodules were also observed in MSCs (Fig. 1*C*). At the same time, after induction of adipogenic differentiation, diffusely distributed red lipid droplets were observed in MSCs (Fig. 1*D*).

MSC-derived exosome pretreatment improves OS injury and inhibits inflammatory response in traumatic ALI rats. Through transmission electron microscopy, it was shown that exosomes derived from MSCs presented as spherical particles with a diameter of 30–50 nm (Fig. 2*A*). The average size of exosomes was detected by nanoparticle tracking analysis and was calculated to be 48.9 nm (Fig. 2*B*). Western blot analysis showed that the exosome markers CD63, CD9, and CD81 were significantly enriched in the exosome (Fig. 2*C*). The timeline of the timeframes between injury and exosome administration is

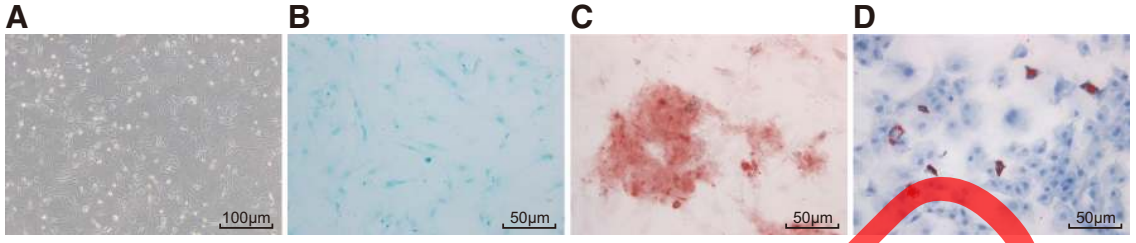

Fig. 1. Morphological changes of mesenchymal stem cells (MSCs). *A*: morphology of primary MSCs (7 days, ×100). *B*: chondrogenic differentiation of MSCs determined by Alcian blue staining (14 days, ×200). *C*: osteogenic differentiation of MSCs determined by Alizarin red staining (14 days, ×200). *D* adipogenic differentiation of MSCs determined by Oil red O staining (14 days, ×200).

shown in Fig. 2*D*. A survival analysis showed that the survival rate of the ALI group was significantly decreased relative to the normal group ($P < 0.05$). Nonetheless, the survival rate of the ALI + exosomes group was significantly increased compared with ALI + PBS group ($P < 0.05$) (Fig. 2*E*). Following a 7-day period, the W/D of the ALI group was found to be significantly increased, relative to the normal group, and was also accompanied with the infiltration of inflammatory cells, congested capillaries, hemorrhage, and thickening of the alveolar walls ($P < 0.05$). Nevertheless, the W/D was reduced in the ALI + exosomes group compared with the ALI + PBS group and the pathological injury of lung tissues was improved ($P < 0.05$) (Fig. 2*F*). Furthermore, less infiltrative inflammatory cells and congested capillaries were observed with reduced hemorrhage and thinner alveolar walls (Fig. 2, *G* and *H*) ($P < 0.05$).

Relative to the normal group, the number of total cells, macrophages, neutrophils, and lymphocytes in the BALF was significantly increased in the ALI group ($P < 0.05$). Relative to the ALI + PBS group, the ALI + exosomes group exhibited a decrease in the number of total cells, macrophages, neutrophils, and lymphocytes in BALF (Fig. 2, *I–K*) ($P < 0.05$). Furthermore, ELISA was employed to detect the levels of the inflammatory factors (TNF-α, IL-6, IL-8, and IL-10). Relative to the normal group, the ALI group displayed an increase in the levels of TNF-α, IL-6, IL-8 ($P < 0.05$). Moreover, relative to the ALI + PBS group, the ALI + exosomes group showed a decrease in the levels of TNF-α, IL-6, and IL-8 and an increase in the IL-10 level ($P < 0.05$; Fig. 2*L*). Furthermore, the MDA and H_2O_2 levels were increased in the ALI group, relative to the normal group, whereas GSH and SOD levels were decreased ($P < 0.05$). Additionally, exosome treatment resulted in opposite trends (Fig. 2, *M–P*). All these results indicated that MSC-derived exosomes to improve OS injuries and inhibit inflammatory response in traumatic ALI rats.

Silenced P2X7 improves OS injury and inhibits inflammatory response in traumatic ALI rats. It was previously demonstrated that the blocking of intracellular transmission receptor axis P2X7 could alleviate ALI in wild-type (WT) and P2X7 knockout mice (11). ALI rats with P2X7 deficiency exhibited a decrease in the pulmonary edema and alveolar protein content and destroyed alveolar epithelial cell protein permeability (35). Moreover, apoptosis of type I alveolar epithelial cells was inhibited and ALI was alleviated as a result of inhibition of the P2X7 receptor (16). In the current study, RT-qPCR and Western blot analysis indicated that the expression of P2X7 in lung tissues was significantly increased in the ALI group compared with the normal group (Fig. 3, *A–C*; $P < 0.05$). Meanwhile, P2X7 expression in lung tissues of the ALI + exosomes group was significantly decreased compared with the ALI + PBS group ($P < 0.05$).

Relative to the vector-NC group, W/D in the P2X7-vector group was significantly increased. However, W/D was reduced in the si-P2X7 group in comparison with the si-NC group (Fig. 3*D*; $P < 0.05$). Compared with the vector-NC group, the P2X7-vector group presented with infiltration of inflammatory cells, congested capillaries, hemorrhage, and thickened alveolar wall ($P < 0.05$). Less infiltration of inflammatory cells, congested capillaries, hemorrhage, and thinner alveolar wall were observed in the si-P2X7 group compared with those in the si-NC group (Fig. 3, *E* and *F*). Compared with the vector-NC group, the number of total cells, macrophages, neutrophils, and lymphocytes in BALF was increased in the P2X7-vector group ($P < 0.05$). However, the si-P2X7 group exhibited opposite trends in comparison with the si-NC group (Fig. 3, *G–I*). In addition, MDA and H_2O_2 levels in the lung tissues of the P2X7-vector group were significantly increased compared with the vector-NC group, whereas the GSH and SOD levels were decreased ($P < 0.05$). Compared with the si-NC group, MDA and H_2O_2 levels in the lung tissues of the si-P2X7 group were significantly decreased, whereas the GSH and SOD levels were increased (Fig. 3, *J–M*; $P < 0.05$).

Compared with the vector-NC group, increased levels of TNF-α, IL-6, and IL-8 and decreased IL-10 level were found in the P2X7-vector group ($P < 0.05$). However, the si-P2X7 group exhibited opposite trends in comparison with the si-NC group (Fig. 3*N*; $P < 0.05$). Our results indicated that silencing of P2X7 improved OS injury and inhibited inflammatory response in traumatic ALI rats.

miR-124-3p directly targets P2X7 and downregulates P2X7. The miRs binding to P2X7 were predicted using bioinformatics target prediction websites, namely, miRDB, TargetScan, and miRWalk. Especially, 11 miRs were obtained using miRDB, 17 miRs with weighted context++ scores ≤0.25 were included in the prediction results of TargetScan, and 284 miR results were obtained in miRWalk. By comparing the above prediction results, four overlapping miRs including rno-miR-409b, rno-miR-124-3p, rno-miR-149-3p, and rno-miR-1956-5p were obtained (Fig. 4*A*). The results from the bioinformatics website identified a specific binding site between the four miRs and the P2X7 sequence (Fig. 4*B*). This particular finding was also confirmed using dual luciferase reporter gene assay. The results revealed that the luciferase activity of WT was decreased in the miR-409b, miR-124-3p-, miR-149-3p-, and miR-1956-5p-transfected groups compared with the oe-NC group (Fig. 4, *C–F*; $P < 0.05$). However, no

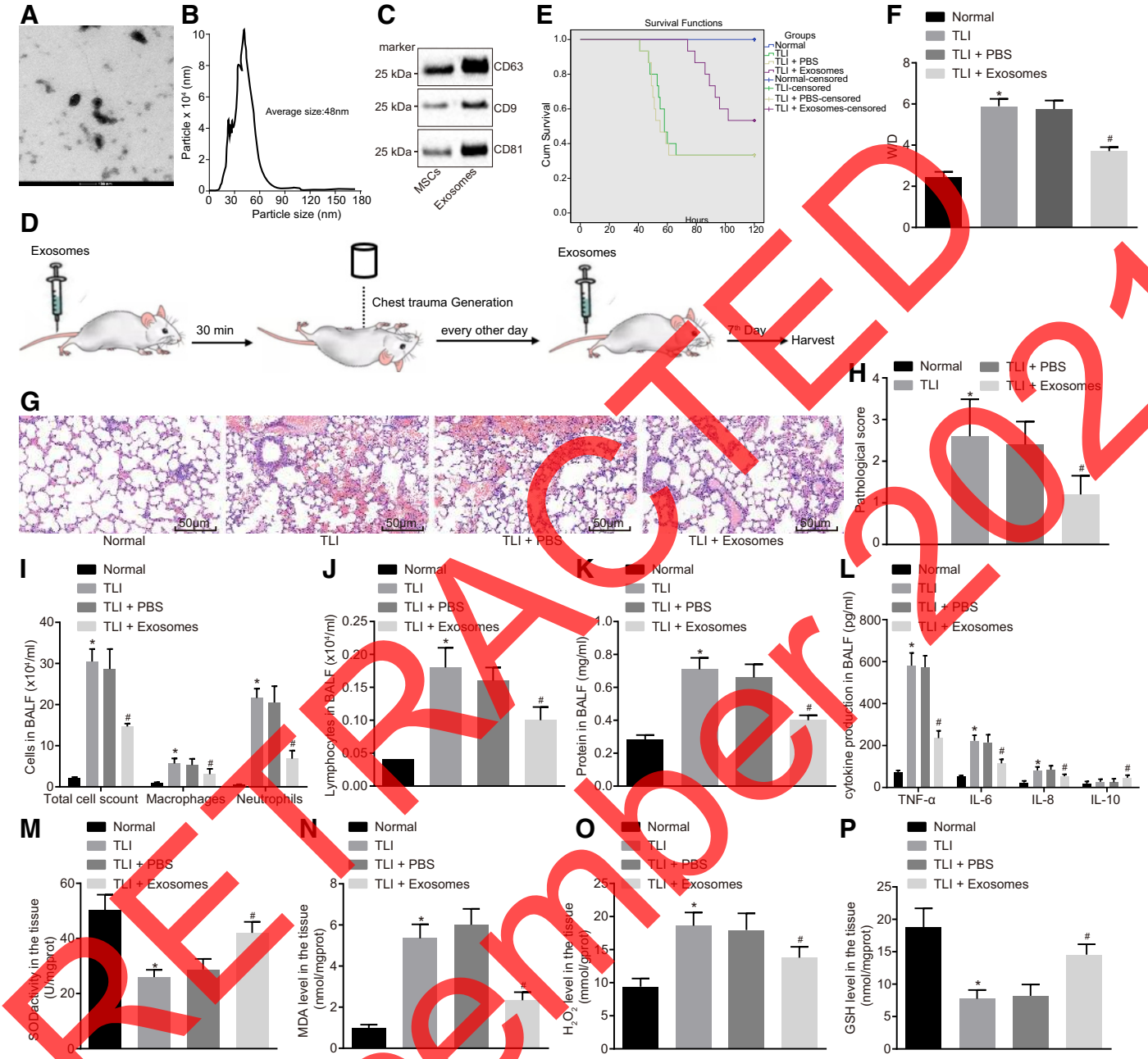

Fig. 2. Mesenchymal stem cell (MSC)-derived exosomes improved oxidative stress injury and inhibited inflammatory response in traumatic acute lung injury (ALI/TLI) rats. *A*: transmission electron microscope imaging of exosomes (×1,000). *B*: nanoparticle tracking analysis of the exosome size. *C*: Western blot analysis of exosome surface markers. *D*: timeline of timeframes between injury and exosome administration. *E*: survival analysis of rats. *F*: ratio of wet weight to dry weight (W/D) in lung tissues. *G* and *H*: pathological changes of lung tissues determined by hematoxylin-eosin staining (×200). *I* and *J*: number of total cells, macrophages, neutrophils, and lymphocytes in bronchoalveolar lavage fluid (BALF). *K*: total protein content in BALF. *L*: levels of tumor necrosis factor-α (TNF-α), interleukin-6 (IL-6), IL-8, and IL-10 detected by ELISA. *M*–*P*: superoxide dismutase (SOD; *M*), methylenedioxyamphetamine (MDA; *N*), H_2O_2 (*O*), and glutathione (GSH; *P*) activity in lung tissues; $n = 15$ in each group. Measurement data are expressed as means ± SD, one-way ANOVA was used for comparison between groups, and the survival rate of 0-120 h in each group was compared by Kaplan-Meier analysis. *$P < 0.05$, compared with normal group; #$P < 0.05$, compared with ALI + PBS group.

differences were observed in the MUT 3′-untranslated region ($P > 0.05$). The above results indicated that miR-409b, miR-124-3p, miR-149-3p, and miR-1956-5p could specifically bind to the P2X7 gene. RT-qPCR results demonstrated that the expression of miR-124-3p in exosomes was much elevated compared with miR-409b (Fig. 4*G*; $P < 0.05$). In addition, P2X7 expression in lung tissues was significantly downregulated in the oe-miR-124-3p group compared with the oe-NC group ($P < 0.05$). However, P2X7 expression in the sh-miR-124-3p group was significantly upregulated compared with the sh-NC group ($P < 0.05$; Fig. 4*H*). In addition, MSCs were transfected with lentiviral miR-124-3p, and the results showed that the oe-miR-24-3p group exhibited approximately fivefold of miR-124-3p expression compared with the oe-NC group.

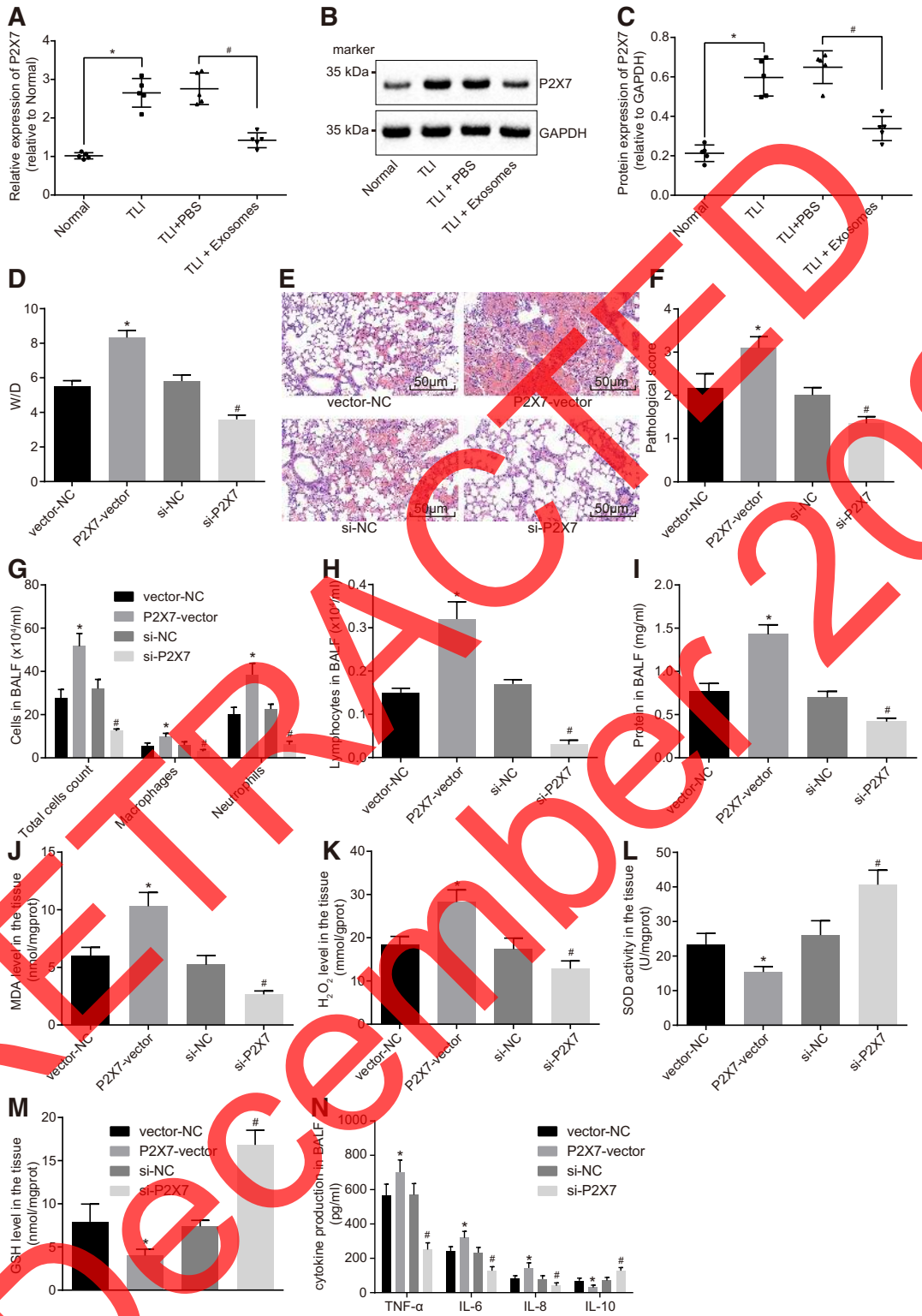

Fig. 3. Silenced P2X ligand-gated ion channel 7 (P2X7) suppressed oxidative stress and inflammatory response in traumatic lung injury (ALI/TLI) rats. *A*: P2X7 mRNA expression in lung tissues after alteration of P2X7 detected by reverse transcription-quantitative polymerase chain reaction (RT-qPCR). *B* and *C*: P2X7 expression in lung tissues after alteration of P2X7 determined by Western blot analysis. *D*: ratio of wet weight to dry weight (W/D) of lung tissues after alteration of P2X7. *E* and *F*: pathological changes in lung tissues after alteration of P2X7 determined by hematoxylin-eosin staining (×200). *G* and *H*: number of total cells, macrophages, neutrophils, and lymphocytes in bronchoalveolar lavage fluid (BALF) after alteration of P2X7. *I*: total protein content in BALF after alteration of P2X7. *J–M*: superoxide dismutase (SOD; *J*), methylenedioxyamphetamine (MDA; *K*), H_2O_2 (*L*), and glutathione (GSH; *M*) activity in lung tissues after alteration of P2X7. *N*: tumor necrosis factor-α (TNF-α), interleukin-6 (IL-6), IL-8, and IL-10 levels after alteration of P2X7 measured by ELISA. Measurement data are expressed as means ± SD, and comparison among multiple groups was performed by one-way ANOVA. $^*P < 0.05$ compared with normal/vector-negative control (NC) group; $\#P < 0.05$, compared with ALI + PBS/si-NC group; $n = 15$ in each group.

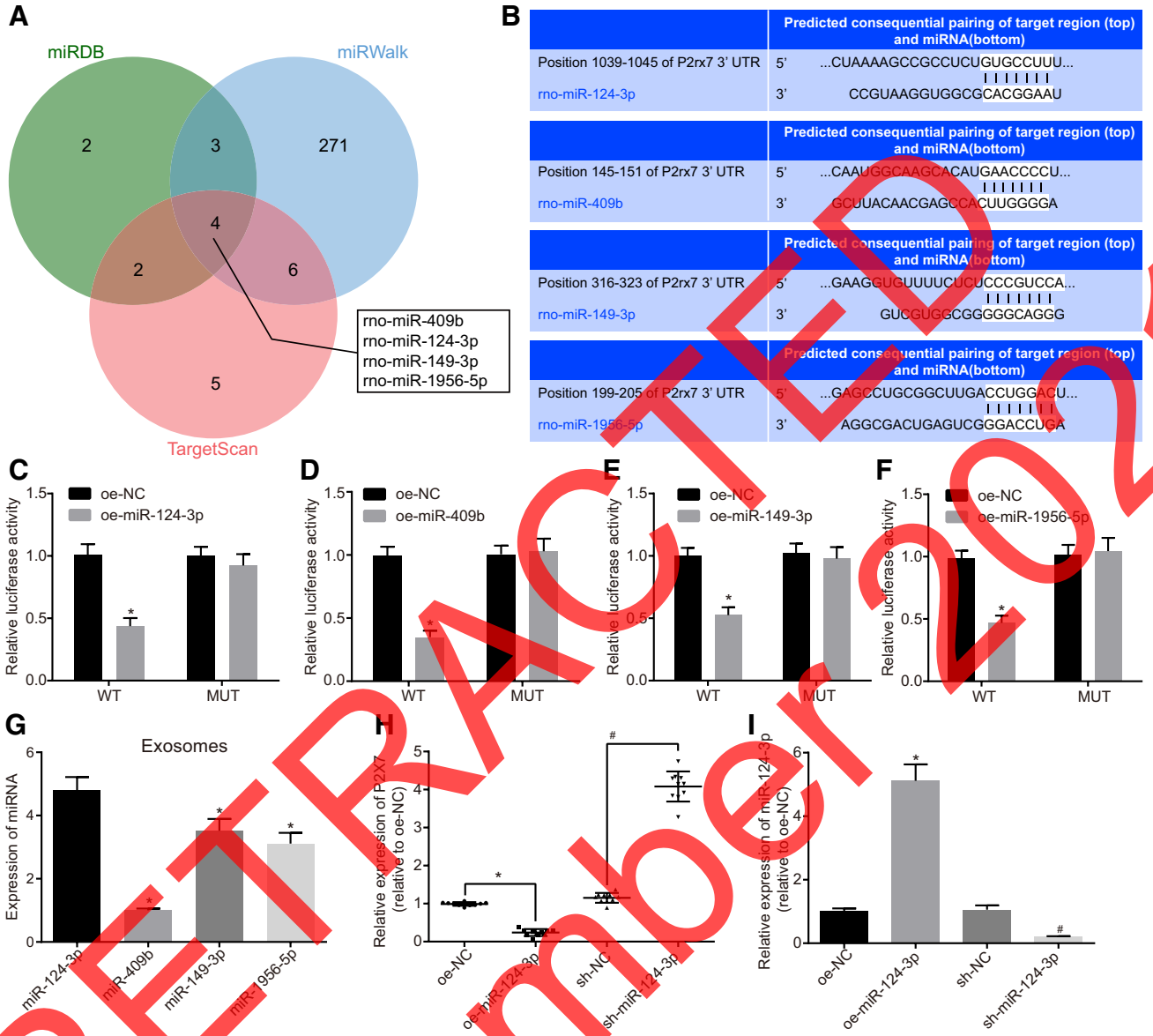

Fig. 4. miR-124-3p targeted P2X ligand-gated ion channel 7 (P2X7) and downregulated P2X7. *A*: prediction of the miRs targeting P2X7 in websites including miRDB, TargetScan, and miRWalk. *B*: prediction of specific binding sites for rno-miR-409b, rno-miR-124-3p, rno-miR-149-3p, and rno-miR-1956-5p with the P2X7 sequence by bioinformatics. *C–F*: dual luciferase reporter gene assay for luciferase activity. WT, wild type; MUT, mutant. $^*P < 0.05$, compared with oe-NC group. *G*: expression of miR-409b, miR-124-3p, miR-149-3p and miR-1956-5p in exosomes detected by reverse transcription-quantitative polymerase chain reaction (RTq-PCR). $^*P < 0.05$, compared with miR-124-3p. *H*: P2X7 expression in lung tissues after alteration of miR-124-3p determined by RT-qPCR. $^*P < 0.05$, compared with the oe-NC group; $^\#P < 0.05$, compared with the sh-NC group. Samples were lung tissues of traumatic acute lung injury rats treated by tail vein injection of miR-124-3p or/and P2X7 vectors. *I*: exosomal miR-124-3p expression from MSCs in the oe-NC, oe-miR-124-3p, sh-NC and sh-miR-124-3p groups detected by RT-qPCR; $n = 15$ in each group. Measurement data are expressed as means ± SD. Cell viability was compared by *t*-test, and one-way ANOVA was used for comparison among multiple groups. The experiment was repeated 3 times.

Compared with the sh-NC group, the sh-miR-124-3p group showed 80% inhibition rate (Fig. 4*I*). The above results demonstrated that P2X7 was a target gene of miR-124-3p and could be downregulated by miR-124-3p.

Exosomal miR-124-3p improves OS injury and inhibits inflammatory response in traumatic ALI rats by downregulating P2X7. In comparison with the oe-NC group, the pathological injury of the lung tissues was found to be alleviated in the oe-miR-124-3p group. Less infiltration of inflammatory cells, congested capillaries, and hemorrhage were observed with thinner alveolar walls ($P < 0.05$). In addition, W/D, MDA, and H_2O_2 levels were also decreased, whereas GSH and SOD levels were increased ($P < 0.05$). Compared with the oe-miR-124-3p + vector-NC group, the oe-miR-124-3p + P2X7-vector group exhibited elevated W/D with increased infiltration of inflammatory cells, congested capillaries and hemorrhage. Furthermore, thickened alveolar walls were also observed, whereas MDA, and H_2O_2 levels were increased and GSH and SOD levels were decreased (Fig. 5, *A–C* and *G–J*; $P < 0.05$).

Compared with oe-NC group, the numbers of total cells, macrophages, neutrophils, and lymphocytes in BALF were found to be decreased in the oe-miR-124-3p group ($P < 0.05$).

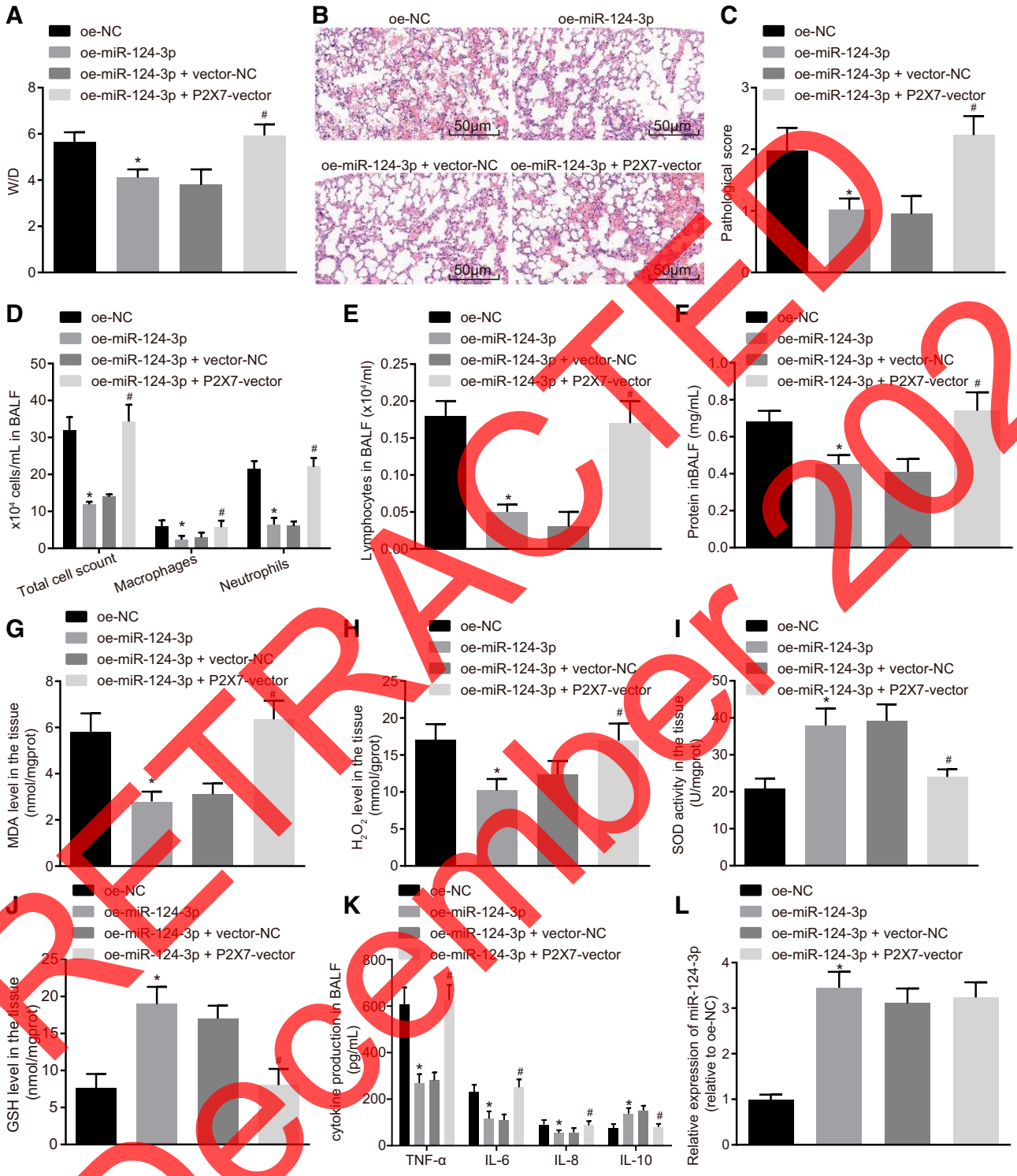

Fig. 5. Exosomal miR-124-3p improved oxidative stress injury and inhibited inflammatory response in traumatic acute lung injury (ALI) rats by downregulating P2X ligand-gated ion channel 7 (P2X7). *A*: ratio of wet weight to dry weight (W/D) in lung tissues after alteration of miR-124-3p and P2X7. *B* and *C*: pathological changes of lung tissues after alteration of miR-124-3p and P2X7 determined by hematoxylin-eosin staining (×200). *D* and *E*: number of total cells, macrophages, neutrophils, and lymphocytes in bronchoalveolar lavage fluid (BALF) after alteration of miR-124-3p and P2X7. Samples were lung tissues of traumatic ALI rats treated by tail vein injection of miR-124-3p or/and P2X7 vectors. *F*: total protein content in BALF after alteration of miR-124-3p and P2X7. *G–J*: superoxide dismutase (SOD; *G*), methylenedioxyamphetamine (MDA; *H*), H_2O_2 (*I*), and glutathione (GSH; *J*) activity in lung tissues after alteration of miR-124-3p and P2X7. *K*: tumor necrosis factor-α (TNF-α), interleukin-6 (IL-6), IL-8, and IL-10 levels determined by ELISA after alteration of miR-124-3p and P2X7. *L*: miR-124-3p expression in lung tissues detected by reverse transcription-quantitative polymerase chain reaction (RT-qPCR). Samples were lung tissues of traumatic ALI rats treated by tail vein injection of miR-124-3p or/and P2X7 vectors; $n = 15$ in each group. Measurement data are expressed by means ± SD, independent sample *t*-test was used for comparison between the 2 groups, and one-way ANOVA was used for comparison between groups. The experiment was repeated 3 times. $^*P < 0.05$, compared with the oe-NC group; $\#P < 0.05$, compared with the oe-miR-124-3p + vector-negative control (NC) group; $n = 5$.

Additionally, decreased total protein content of inflammatory factors was noted in the oe-miR-124-3p group. Compared with the oe-miR-124-3p + vector-NC group, the oe-miR-124-3p + P2X7-vector group exhibited a higher number of total cells, macrophages, neutrophils, and lymphocytes in BALF accompanied by increased total protein content of inflammatory factors (Fig. 5, *D–F*; $P < 0.05$). ELISA was used to detected levels of inflammatory factors, and the results showed that compared with the oe-NC group, the levels of TNF-α, IL-6, and IL-8 were decreased and IL-10 level was increased in lung tissues in the oe-miR-124-3p group. Compared with the oe-miR-124-3p + vector-NC group, the levels of TNF-α, IL-6, and IL-8 were increased and IL-10 level was decreased in the oe-miR-124-3p + P2X7-vector group (Fig. 5*K*; $P < 0.05$). Furthermore, RT-qPCR was employed to detect the expression of miR-124-3p, and the results revealed that compared with the oe-NC group, the expression of miR-124-3p was increased approximately three times in the oe-miR-124-3p group, oe-miR-124-3p + vector-NC group, and oe-miR-124-3p + P2X7-vector group. There were no significant differences between the oe-miR-124-3p + vector-NC group and oe-miR-124-3p + P2X7-vector group (Fig. 5*L*). The above results demonstrated that exosomal miR-124-3p improved OS injury and inhibited inflammatory response in traumatic ALI rats by downregulating P2X7.

DISCUSSION

Lung injury may be caused by systemic injury or inhalation of oropharyngeal contaminants (41). It has been demonstrated that miR-124-3p is capable of preventing excessive inflammatory response by inhibiting the Toll-like receptor pathway (20). Moreover, the findings of a previous study revealed that P2X7 with abundant expression in immune cells can serve as a target biomarker for the treatment of inflammatory diseases (46). Thus this present study aimed to determine the role of miR-124-3p and P2X7 in ALI, and the key findings indicated that miR-124-3p transferred by MSC-derived exosomes inhibits the expression of P2X7, thus alleviating OS injury and inflammatory response in rats with traumatic ALI.

Initially, the current study revealed that the expression of P2X7 was upregulated in traumatic ALI rats and miR-124-3p was overexpressed in MSC-derived exosomes. A previous study found that downregulation of P2X7 inhibited inflammation and alleviated ALI (11). Interestingly, another study also proved that decreased expression of P2X7 in ALI can attenuate inflammation (8). Notably, it has been well established that exosomes can be derived from MSCs (13). In addition, consistent with our results, miR-124-3p was found to be increased in exosomes after the occurrence of TBI (21). In this study, we performed dual luciferase assay, which revealed that miR-124-3p could target P2X7 to inhibit its expression. It has been demonstrated that miR-124-3p plays a role in posttranscriptional regulation of gene expression and has been further demonstrated to reduce luciferase activity in C/EBPa, indicating that miR-124-3p could directly bind to C/EBPa (32). Furthermore, the expression of P2X7 is correlated with different miRs such as miR-186 and miR-150 (50).

Additionally, a key finding of this study was that MSC-derived exosomes, exosomal miR-124-3p and P2X7 silencing exerted an inhibitory effect on OS in traumatic ALI rats, characterized by decreased MDA and increased GSH and SOD levels. ALI induced by TBI is exhibited by several pathological changes including cell apoptosis, OS injury, and inflammatory response (45). MDA, GSH, and SOD are reported to be key parameters of OS (29). In line with our study, it has been proven that when OS was alleviated, the level of MDA was decreased but GSH content and SOD activity were increased (36). In addition, miRs have been reported to play a vital role in the synthesis of GSH via the regulation of related genes (34). Strikingly, a previous study indicated that exosomes derived from MSCs can inhibit OS (4). More specifically, findings from a prior study highlighted that miR-124-3p was downregulated in OS (44). Furthermore, inhibition of P2X7 can alleviate OS as well (49). All these findings support our results that exosomal miR-124-3p and silencing of P2X7 can suppress OS in traumatic ALI rats.

Subsequently, the current study also found that MSC-derived exosomes, exosomal miR-124-3p, and P2X7 silencing attenuated inflammatory response in traumatic ALI rats with decreased levels of TNF-α, IL-6, and IL-8 as well as increased IL-10 level. It has been reported that biomarkers of systemic inflammation, such as IL-10, TNF-α, and IL-8, are broadly used in diagnoses of ALI (39). Consistent with our study, it has been shown that TNF-α, an initiating cytokine in ALI induced by extracorporeal circulation, release could be induced by P2X7 through increasing the activity of TNF-α-converting enzyme (6, 22). Moreover, a previous study provided evidence that miR-124-3p can decrease the expression levels of inflammatory factors including TNF-α and IL-1 (12). It has also been confirmed that the expression of many inflammatory factors including IL-6 and IL-8 can be regulated by P2X7 (48). More specifically, a previous study proved that P2X7 can upregulate the expression of IL-6 (26). Another study also indicated that

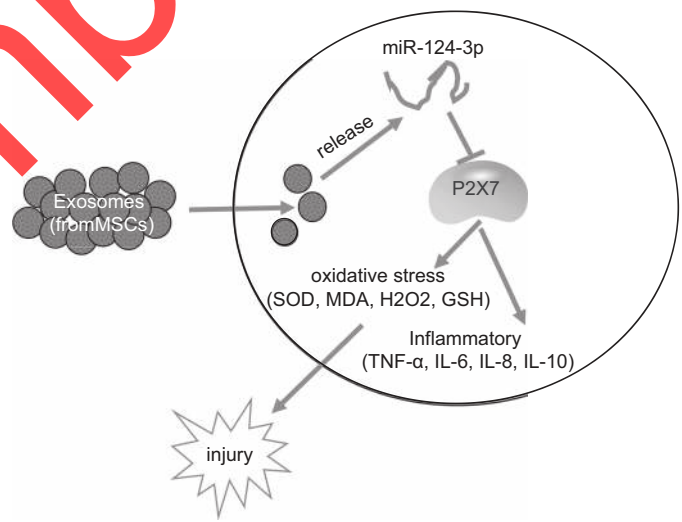

Fig. 6. Mesenchymal stem cell-derived exosomal miR-124-3p inhibits P2X ligand-gated ion channel 7 (P2X7) expression and alleviates oxidative stress and inflammatory response in traumatic acute lung injury rats. Rat MSC-derived exosomes are rich in miR-124-3p. Exosomes help miR-124-3p to bind to P2X7 and inhibit P2X7 expression, which can reduce the activity of methylenedioxyamphetamine (MDA) and H_2O_2 and levels of inflammatory factors including tumor necrosis factor-α (TNF-α), interleukin-6 (IL-6), IL-8, and IL-10 but promote superoxide dismutase (SOD) and glutathione (GSH) activity, thereby preventively alleviating oxidative stress injury and inflammatory response in rats with traumatic ALI induced by P2X7.

genistin may play an antioxidant and anti-inflammatory role in cardioprotection via silencing of P2X7 (15). In addition, previous findings confirmed that elevated exosomes can reduce the expression of TNF-α and IL-6 (7), indicating alleviation of the inflammatory response.

Based on previous findings, the current study concludes that miR-124-3p transferred by MSC-derived exosome pretreatment inhibits the expression of P2X7 and alleviates OS injury and inflammatory response in rats with traumatic ALI (Fig. 6). These findings identified miR-124-3p and P2X7 as potential therapeutic targets for the treatment of ALI. However, limited conditions to detect the biodistribution of exosomes and lentiviral vectors in vivo remain to be the limitations of our study. Further research focusing on the biodistribution of exosomes and lentiviral vectors is warranted to further elucidate the mechanisms in this study. Several studieshave shown that P2X7 was correlated with alveolar epithelial cells (11, 16, 35). Therefore, we hypothesized that alveolar epithelial cells might be the major recipient of the exosomes and lentiviral vectors, and further efforts need to focus on solving this problem. Moreover, considering that trauma by its nature cannot be predicted, the animal treatment could be improved by doing an additional series experiments to treated animals with exosomes after chest injury.

GRANTS

This study was supported by Department of Science and Technology of Jilin Province (No. 20190701068GH).

DISCLOSURES

No conflicts of interest, financial or otherwise, are declared by the authors.

AUTHOR CONTRIBUTIONS

Q.-C.L. and Y.L. conceived and designed research; Q.-C.L. performed experiments; Y.L. analyzed data; Y.L. interpreted results of experiments; Q.-C.L. prepared figures; Y.L. and Z.-B.S. drafted manuscript; Z.-B.S. edited and revised manuscript; Q.-C.L., Y.L., and Z.-B.S. approved final version of manuscript.

REFERENCES

1. **Ahmad SB, Menaker J, Kufera J, O'Connor J, Scalea TM, Stein DM.** Extracorporeal membrane oxygenation after traumatic injury. *J Trauma Acute Care Surg* 82: 587–591, 2017. doi:10.1097/TA.0000000000001352.
2. **Aliotta JM, Pereira M, Wen S, Dooner MS, Del Tatto M, Papa E, Goldberg LR, Baird GL, Ventetuolo CE, Quesenberry PJ, Klinger JR.** Exosomes induce and reverse monocrotaline-induced pulmonary hypertension in mice. *Cardiovasc Res* 110: 319–330, 2016. doi:10.1093/cvr/cvw054.
3. **Alvarez-Erviti L, Seow Y, Yin H, Betts C, Lakhal S, Wood MJ.** Delivery of siRNA to the mouse brain by systemic injection of targeted exosomes. *Nat Biotechnol* 29: 341–345, 2011. doi:10.1038/nbt.1807.
4. **Arslan F, Lai RC, Smeets MB, Akeroyd L, Choo A, Aguor EN, Timmers L, van Rijen HV, Doevendans PA, Pasterkamp G, Lim SK, de Kleijn DP.** Mesenchymal stem cell-derived exosomes increase ATP levels, decrease oxidative stress and activate PI3K/Akt pathway to enhance myocardial viability and prevent adverse remodeling after myocardial ischemia/reperfusion injury. *Stem Cell Res (Amst)* 10: 301–312, 2013. doi:10.1016/j.scr.2013.01.002.
5. **Arulkumaran N, Unwin RJ, Tam FW.** A potential therapeutic role for P2X7 receptor (P2X7R) antagonists in the treatment of inflammatory diseases. *Expert Opin Investig Drugs* 20: 897–915, 2011. doi:10.1517/13543784.2011.578068.
6. **Barberà-Cremades M, Gómez AI, Baroja-Mazo A, Martínez-Alarcón L, Martínez CM, de Torre-Minguela C, Pelegrín P.** P2X7 receptor induces tumor necrosis factor-α converting enzyme activation and release to boost TNF-α production. *Front Immunol* 8: 862, 2017. doi:10.3389/fimmu.2017.00862.
7. **Beninson LA, Fleshner M.** Exosomes in fetal bovine serum dampen primary macrophage IL-1β response to lipopolysaccharide (LPS) challenge. *Immunol Lett* 163: 187–192, 2015. doi:10.1016/j.imlet.2014.10.019.
8. **Cai Z, Liu J, Bian H, Cai J, Zhu G.** Suppression of P2X7/NF-κB pathways by Schisandrin B contributes to attenuation of lipopolysaccharide-induced inflammatory responses in acute lung injury. *Arch Pharm Res* 39: 499–507, 2016. doi:10.1007/s12272-016-0713-0.
9. **El Agha E, Kramann R, Schneider RK, Li X, Seeger W, Humphreys BD, Bellusci S.** Mesenchymal stem cells in fibrotic disease. *Cell Stem Cell* 21: 166–177, 2017. doi:10.1016/j.stem.2017.07.011.
10. **Farooq RK, Tanti A, Ainouche S, Roger S, Belzung C, Camus V.** A P2X7 receptor antagonist reverses behavioural alterations, microglial activation and neuroendocrine dysregulation in an unpredictable chronic mild stress (UCMS) model of depression in mice. *Psychoneuroendocrinology* 97: 120–130, 2018. doi:10.1016/j.psyneuen.2018.07.016.
11. **Galam L, Rajan A, Failla A, Soundararajan R, Lockey RF, Kolliputi N.** Deletion of P2X7 attenuates hyperoxia-induced acute lung injury via inflammasome suppression. *Am J Physiol Lung Cell Mol Physiol* 310: L572–L581, 2016. doi:10.1152/ajplung.00417.2015.
12. **Geng L, Liu W, Chen Y.** miR-124-3p attenuates MPP^+-induced neuronal injury by targeting STAT3 in SH-SY5Y cells. *Exp Biol Med (Maywood)* 242: 1757–1764, 2017. doi:10.1177/1535370217734492.
13. **Goodarzi P, Larijani B, Alavi-Moghadam S, Tayanloo-Beik A, Mohamadi-Jahani F, Ranjbaran N, Payab M, Falahzadeh K, Mousavi M, Arjmand B.** Mesenchymal stem cells-derived exosomes for wound regeneration. *Adv Exp Med Biol* 1119: 119–131, 2018. doi:10.1007/5584_2018_251.
14. **Gore AV, Bible LE, Livingston DH, Mohr AM, Sifri ZC.** Can mesenchymal stem cells reverse chronic stress-induced impairment of lung healing following traumatic injury? *J Trauma Acute Care Surg* 78: 767–772, 2015. doi:10.1097/TA.0000000000000592.
15. **Gu M, Zheng AB, Jin J, Cui Y, Zhang N, Che ZP, Wang Y, Zhan J, Tu WJ.** Cardioprotective effects of genistin in rat myocardial ischemia-reperfusion injury studies by regulation of P2X7/NF-κB pathway. *Evid Based Complement Alternat Med* 2016: 5381290, 2016. doi:10.1155/2016/5381290.
16. **Guo Y, Mishra A, Weng T, Chintagari NR, Wang Y, Zhao C, Huang C, Liu L.** Wnt3a mitigates acute lung injury by reducing P2X7 receptor-mediated alveolar epithelial type I cell death. *Cell Death Dis* 5: e1286, 2014. doi:10.1038/cddis.2014.254.
17. **Hayes M, Curley G, Ansari B, Laffey JG.** Clinical review: stem cell therapies for acute lung injury/acute respiratory distress syndrome–hope or hype? *Crit Care* 16: 205, 2012. doi:10.1186/cc10570.
18. **Hoth JJ, Wells JD, Jones SE, Yoza BK, McCall CE.** Complement mediates a primed inflammatory response after traumatic lung injury. *J Trauma Acute Care Surg* 76: 601–608, 2014. doi:10.1097/TA.0000000000000129.
19. **Hu LY, Cui JB, Xu XM, Huang ZH, Jiao HT.** Expression of Nrf2-Keap1-ARE signal pathway in traumatic lung injury and functional study. *Eur Rev Med Pharmacol Sci* 22: 1402–1408, 2018. doi:10.26355/eurrev_201803_14486.
20. **Huang L, Ma J, Sun Y, Lv Y, Lin W, Liu M, Tu C, Zhou P, Gu W, Su S, Zhang G.** Altered splenic miRNA expression profile in H1N1 swine influenza. *Arch Virol* 160: 979–985, 2015. doi:10.1007/s00705-015-2351-0.
21. **Huang S, Ge X, Yu J, Han Z, Yin Z, Li Y, Chen F, Wang H, Zhang J, Lei P.** Increased miR-124-3p in microglial exosomes following traumatic brain injury inhibits neuronal inflammation and contributes to neurite outgrowth *via* their transfer into neurons. *FASEB J* 32: 512–528, 2018. doi:10.1096/fj.201700673R.
22. **Li T, Luo N, Du L, Zhou J, Zhang J, Gong L, Jiang N.** Tumor necrosis factor-α plays an initiating role in extracorporeal circulation-induced acute lung injury. *Lung* 191: 207–214, 2013. doi:10.1007/s00408-012-9449-x.
23. **Liu F, Hu H, Zhao J, Zhang Z, Ai X, Tang L, Xie L.** miR-124-3p acts as a potential marker and suppresses tumor growth in gastric cancer. *Biomed Rep* 9: 147–155, 2018. doi:10.3892/br.2018.1113.
24. **Liu Y, Lu J, Wang X, Chen L, Liu S, Zhang Z, Yao W.** Erythropoietin-derived peptide protects against acute lung injury after rat traumatic brain injury. *Cell Physiol Biochem* 41: 2037–2044, 2017. doi:10.1159/000475434.

25. **Livak KJ, Schmittgen TD.** Analysis of relative gene expression data using real-time quantitative PCR and the 2(-delta C(T)) method. *Methods* 25: 402–408, 2001. doi:10.1006/meth.2001.1262.
26. **Lu W, Albalawi F, Beckel JM, Lim JC, Laties AM, Mitchell CH.** The P2X7 receptor links mechanical strain to cytokine IL-6 up-regulation and release in neurons and astrocytes. *J Neurochem* 141: 436–448, 2017. doi:10.1111/jnc.13998.
27. **Ma B, Yang JY, Song WJ, Ding R, Zhang ZC, Ji HC, Zhang X, Wang JL, Yang XS, Tao KS, Dou KF, Li X.** Combining exosomes derived from immature DCs with donor antigen-specific treg cells induces tolerance in a rat liver allograft model. *Sci Rep* 6: 32971, 2016. doi:10.1038/srep32971.
28. **Ma J, Zhao Y, Sun L, Sun X, Zhao X, Sun X, Qian H, Xu W, Zhu W.** Exosomes derived from Akt-modified human umbilical cord mesenchymal stem cells improve cardiac regeneration and promote angiogenesis via activating platelet-derived growth factor D. *Stem Cells Transl Med* 6: 51–59, 2017. doi:10.5966/sctm.2016-0038.
29. **Moniruzzaman M, Mukherjee J, Jacquin L, Mukherjee D, Mitra P, Ray S, Chakraborty SB.** Physiological and behavioural responses to acid and osmotic stress and effects of Mucuna extract in guppies. *Ecotoxicol Environ Saf* 163: 37–46, 2018. doi:10.1016/j.ecoenv.2018.07.053.
30. **Nojehdehi S, Soudi S, Hesampour A, Rasouli S, Soleimani M, Hashemi SM.** Immunomodulatory effects of mesenchymal stem cell-derived exosomes on experimental type-1 autoimmune diabetes. *J Cell Biochem* 119: 9433–9443, 2018. doi:10.1002/jcb.27260.
31. **Nong K, Wang W, Niu X, Hu B, Ma C, Bai Y, Wu B, Wang Y, Ai K.** Hepatoprotective effect of exosomes from human-induced pluripotent stem cell-derived mesenchymal stromal cells against hepatic ischemia-reperfusion injury in rats. *Cytotherapy* 18: 1548–1559, 2016. doi:10.1016/j.jcyt.2016.08.002.
32. **Pan Y, Jing J, Qiao L, Liu J, An L, Li B, Ren D, Liu W.** MiRNA-seq reveals that miR-124-3p inhibits adipogenic differentiation of the stromal vascular fraction in sheep via targeting C/EBPα. *Domest Anim Endocrinol* 65: 17–23, 2018. doi:10.1016/j.domaniend.2018.05.002.
33. **Raghavendran K, Davidson BA, Helinski JD, Marschke CJ, Manderscheid P, Woytash JA, Notter RH, Knight PR.** A rat model for isolated bilateral lung contusion from blunt chest trauma. *Anesth Analg* 101: 1482–1489, 2005. doi:10.1213/01.ANE.0000180201.25746.1F.
34. **Ren X, Gaile DP, Gong Z, Qiu W, Ge Y, Zhang C, Huang C, Yan H, Olson JR, Kavanagh TJ, Wu H.** Arsenic responsive microRNAs in vivo and their potential involvement in arsenic-induced oxidative stress. *Toxicol Appl Pharmacol* 283: 198–209, 2015. doi:10.1016/j.taap.2015.01.014.
35. **Riteau N, Gasse P, Fauconnier L, Gombault A, Couegnat M, Fick L, Kanellopoulos J, Quesniaux VF, Marchand-Adam S, Crestani B, Ryffel B, Couillin I.** Extracellular ATP is a danger signal activating P2X7 receptor in lung inflammation and fibrosis. *Am J Respir Crit Care Med* 182: 774–783, 2010. doi:10.1164/rccm.201003-0359OC.
36. **Sayed DA, Soliman AM, Fahmy SR.** Echinochrome pigment as novel therapeutic agent against experimentally–induced gastric ulcer in rats. *Biomed Pharmacother* 107: 90–95, 2018. doi:10.1016/j.biopha.2018.07.173.
37. **Shamili FH, Bayegi HR, Salmasi Z, Sadri K, Mahmoudi M, Kalantari M, Ramezani M, Abnous K.** Exosomes derived from TRAIL-engineered mesenchymal stem cells with effective anti-tumor activity in a mouse melanoma model. *Int J Pharm* 549: 218–229, 2018. doi:10.1016/j.ijpharm.2018.07.067.
38. **Shieh CH, Heinrich A, Serchov T, van Calker D, Biber K.** P2X7-dependent, but differentially regulated release of IL-6, CCL2, and TNF-α in cultured mouse microglia. *Glia* 62: 592–607, 2014. doi:10.1002/glia.22628.
39. **Störmann P, Lustenberger T, Relja B, Marzi I, Wutzler S.** Role of biomarkers in acute traumatic lung injury. *Injury* 48: 2400–2406, 2017. doi:10.1016/j.injury.2017.08.041.
40. **Tong L, Zhou J, Rong L, Seeley EJ, Pan J, Zhu X, Liu J, Wang Q, Tang X, Qu J, Bai C, Song Y.** Fibroblast growth factor-10 (FGF-10) mobilizes lung-resident mesenchymal stem cells and protects against acute lung injury. *Sci Rep* 6: 21642, 2016. doi:10.1038/srep21642.
41. **van den Boogaard FE, Hofstra JJ, Brands X, Levi MM, Roelofs JJ, Zaat SA, Van't Veer C, van der Poll T, Schultz MJ.** Nebulized recombinant human tissue factor pathway inhibitor attenuates coagulation and exerts modest anti-inflammatory effects in rat models of lung injury. *J Aerosol Med Pulm Drug Deliv* 30: 91–99, 2017. doi:10.1089/jamp.2016.1317.
42. **Wang Y, Chen L, Wu Z, Wang M, Jin F, Wang N, Hu X, Liu Z, Zhang CY, Zen K, Chen J, Liang H, Zhang Y, Chen X.** miR-124-3p functions as a tumor suppressor in breast cancer by targeting CBL. *BMC Cancer* 16: 826, 2016. doi:10.1186/s12885-016-2862-4.
43. **Wong SP, Rowley JE, Redpath AN, Tilman JD, Fellous TG, Johnson JR.** Pericytes, mesenchymal stem cells and their contributions to tissue repair. *Pharmacol Ther* 151: 107–120, 2015. doi:10.1016/j.pharmthera.2015.03.006.
44. **Wu C, Liu Z, Ma L, Pei C, Qin L, Gao N, Li J, Yin Y.** MiRNAs regulate oxidative stress related genes via binding to the 3′ UTR and TATA-box regions: a new hypothesis for cataract pathogenesis. *BMC Ophthalmol* 17: 142, 2017. doi:10.1186/s12886-017-0537-9.
45. **Xu X, Zhi T, Chao H, Jiang K, Liu Y, Bao Z, Fan L, Wang D, Li Z, Liu N, Ji J.** ERK1/2/mTOR/Stat3 pathway-mediated autophagy alleviates traumatic brain injury-induced acute lung injury. *Biochim Biophys Acta Mol Basis Dis* 1864, *5 Pt A*: 1663–1674, 2018. doi:10.1016/j.bbadis.2018.02.011.
46. **Young CNJ, Górecki DC.** P2RX7 purinoceptor as a therapeutic target-the second coming? *Front Chem* 6: 248, 2018. doi:10.3389/fchem.2018.00248.
47. **Zhang D, Lee H, Zhu Z, Minhas JK, Jin Y.** Enrichment of selective miRNAs in exosomes and delivery of exosomal miRNAs in vitro and in vivo. *Am J Physiol Lung Cell Mol Physiol* 312: L110–L121, 2017. doi:10.1152/ajplung.00423.2016.
48. **Zhang W, Zhong B, Zhang C, Luo C, Zhan Y.** miR-373 regulates inflammatory cytokine-mediated chondrocyte proliferation in osteoarthritis by targeting the P2X7 receptor. *FEBS Open Bio* 8: 325–331, 2018. doi:10.1002/2211-5463.12345.
49. **Zhang Y, Yuan F, Cao X, Zhai Z, GangHuang, Du X, Wang Y, Zhang J, Huang Y, Zhao J, Hou W.** P2X7 receptor blockade protects against cisplatin-induced nephrotoxicity in mice by decreasing the activities of inflammasome components, oxidative stress and caspase-3. *Toxicol Appl Pharmacol* 281: 1–10, 2014. doi:10.1016/j.taap.2014.09.016.
50. **Zhou L, Qi X, Potashkin JA, Abdul-Karim FW, Gorodeski GI.** MicroRNAs miR-186 and miR-150 down-regulate expression of the pro-apoptotic purinergic P2X7 receptor by activation of instability sites at the 3′-untranslated region of the gene that decrease steady-state levels of the transcript. *J Biol Chem* 283: 28274–28286, 2008. doi:10.1074/jbc.M802663200.
51. **Zhou Z, You Z.** Mesenchymal stem cells alleviate LPS-induced acute lung injury in mice by MiR-142a-5p-controlled pulmonary endothelial cell autophagy. *Cell Physiol Biochem* 38: 258–266, 2016. doi:10.1159/000438627.